


## Spatiotemporal Impact Analysis of Land Surface Temperature Variations: A Case Study of the Northeastern Part of Baghdad Province, Iraq (2000-2024)

Basheer S. Jasim

*Technical Institute of Babylon, Al-Furat Al-Awsat Technical University, Iraq*

Follow this and additional works at: <https://bjeps.alkafeel.edu.iq/journal>

 Part of the [Civil Engineering Commons](#), [Environmental Engineering Commons](#), and the [Other Civil and Environmental Engineering Commons](#)

### Recommended Citation

Jasim, Basheer S. (2025) "Spatiotemporal Impact Analysis of Land Surface Temperature Variations: A Case Study of the Northeastern Part of Baghdad Province, Iraq (2000-2024)," *Al-Bahir*. Vol. 6: Iss. 1, Article 2.

Available at: <https://doi.org/10.55810/2313-0083.1081>

This Original Study is brought to you for free and open access by Al-Bahir. It has been accepted for inclusion in Al-Bahir by an authorized editor of Al-Bahir. For more information, please contact [bjeps@alkafeel.edu.iq](mailto:bjeps@alkafeel.edu.iq).

---

# Spatiotemporal Impact Analysis of Land Surface Temperature Variations: A Case Study of the Northeastern Part of Baghdad Province, Iraq (2000-2024)

## Source of Funding

No Funding.

## Conflict of Interest

No conflicts of interest related to this work.

## Data Availability

Publicly available data.

## Author Contributions

The author declares sole responsibility for all aspects of this research. This includes data collection, analysis, and interpretation, as well as the drafting and revision of the manuscript.

## ORIGINAL STUDY

# Spatiotemporal Impact Analysis of Land Surface Temperature Variations: A Case Study of the Northeastern Part of Baghdad Province, Iraq (2000–2024)

Basheer S. Jasim

Technical Institute of Babylon, Al-Furat Al-Awsat Technical University, Iraq

## Abstract

Land Surface Temperature maps are handy tools in a wide variety of scientific and practical fields. Monitoring climate change, researching the consequences of global warming, and evaluating the health of ecosystems are some of the applications that are used extensively. In addition, they have uses in agriculture, such as determining the amount of water that vegetation needs and monitoring agricultural regions that are experiencing drought. This study utilized a remote sensing approach to estimate land surface temperature with Landsat imagery from two periods, respectively, 2000 and 2024. The Landsat user's guide provided the algorithm to convert the images from DN to TOA radiance. Almost all stations show a significant increase in LST from 2000 to 2024. Some stations show significant increases of more than 10 °C. RMSE slightly increased from 1.89 to 1.98, indicating minor forecast inaccuracies. The average temperature rose from 34.76 °C to 40.25 °C, with maximum temperatures increasing from 41.14 °C to 48.13 °C and minimum temperatures from 26.29 °C to 33.66 °C. The standard deviation increased from 3.57 to 3.92, indicating greater temperature variability. These findings suggest notable climate changes and support the global warming hypothesis. The general increase in Earth's surface temperatures indicates the effects of global warming and climate change at the local scale. Noticeable increases may be due to urbanization, deforestation, and changes in land use.

**Keywords:** Climate change, Land use land cover dynamics, Land surface temperature, Normalized Difference Vegetation Index (NDVI), Baghdad province

## 1. Introduction

Satellites and other forms of remote sensing provide a treasure trove of data for studying the geographical and temporal variability of environmental parameters [1,2]. Changing land surface temperatures (LSTs) are a major contributor to climate change on a worldwide scale. LST maps help urban planning by analyzing urban heat islands, which helps design green areas and reduce city heat impacts. An estimated 68 % of the world's population will live in urban areas by 2050, up from 30 % in 1950 and 55 % in 2018 [3]. Approximately 97 % of manufactured CO<sub>2</sub> emissions in the 1990s came from only 2 % of the world's geographical

area, proving that urbanization is a significant contributor to climate change on a worldwide scale [4]. Cities are often warmer than their rural counterparts due to urban heat islands, which result from changes in land cover brought about by increased human settlement [5]. Drought, ozone depletion, skin and lung illnesses, and adverse effects on agricultural output are all consequences of abnormal LST [6]. The interaction between the environment's biotic and abiotic components may be better understood using LST estimates across the Earth's surface [6].

The temperature at a particular location on Earth's surface is known as land surface temperature (LST) [7]. The fields of meteorology and climatology have

---

Received 2 September 2024; revised 16 November 2024; accepted 18 November 2024.

Available online 17 January 2025

E-mail address: [basheer.jasim@atu.edu.iq](mailto:basheer.jasim@atu.edu.iq).

<https://doi.org/10.55810/2313-0083.1081>

2313-0083/© 2025 University of AlKafeel. This is an open access article under the CC-BY-NC license (<http://creativecommons.org/licenses/by-nc/4.0/>).

used remote sensing to estimate surface temperature [8]. The current rate of climate change and human activity makes it impossible to ignore changes in land cover. For instance, volcanic eruptions, tsunamis, and disturbances induced by humans are particularly harmful to island ecosystems' flora. In vegetation, seasonal changes are frequent. However, it is also affected by climate change and may undergo significant transformations due to natural catastrophes [9]. Rapid urbanization, driven by rising populations, is a major contributor to the changing global environment, surface cover, urban geometry, and urban climate [10]. Change detection entails quantitatively analyzing the phenomenon's temporal consequences using multi-temporal datasets [11,12].

Cici Alexander [5] key findings include a 3.96 °C difference between urban and rural areas, with strong correlations between LST and specific spectral indices (NIR and SWIR2). Tree cover negatively correlates with LST more than overall vegetation, and tree/building cover variations can explain up to 68 % of LST changes, suggesting potential for climate adaptation through land cover management.

Richard and Ibochi [6] study uses remote sensing to estimate LST, Normalized Difference Vegetation Index (NDVI), and Green Normalized Difference Vegetation Index (GNDVI) for Port Harcourt, Nigeria, comparing data from 1990 to 2017. Landsat imagery analysis revealed the highest LSTs of 28.77 °C in 1990 and 29.37 °C in 2017, with temperature increases linked to urbanization and industrialization. Correlations between LST and NDVI/GNDVI were positive, suggesting remote sensing and GIS are effective for environmental studies.

Researchers now have cutting-edge tools for data-aided environmental management thanks to the combination of GIS and remote sensing technologies [13,14]. As a result of increased human activity and fast urbanization, the surface temperatures in the northeastern portion of Baghdad Province are changing dramatically. Because of this, noticeable changes have occurred in the environment, including the urban heat island effect, the loss of vegetation cover, and the acceleration of desertification. Furthermore, these changes are being compounded by global climate change, leaving the area susceptible to even more variations in surface temperatures. Consequently, this study's primary objective is to examine the changes mentioned above in surface temperatures across space and time from 2000 to 2024 in order to comprehend their possible social and environmental effects, pinpoint the regions most at risk of adverse changes, and ultimately enhance ecological policies.

This research aims to learn how land cover affects LST, identify regions that are abnormally hot or cold, and comprehend the spatial pattern of LST in the research region. To better adapt to climate change and enhance people's living circumstances, urban areas might benefit from understanding the variables that cause the LST phenomenon to rise or decrease.

## 2. Materials and methods

### 2.1. Study area

The study area is located in the northeastern part of Baghdad province, Iraq, an area characterized by its geographical diversity, as it contains urban and agricultural areas. Diyala province forms its eastern boundary, while the major cities of Baghdad province form its western one. It is strategically located near the Diyala River, a major water supply in the area, and the land it drains is vital for agriculture. The degradation of certain agricultural fields and their conversion into residential and industrial zones have been caused by the fast urbanization of this region, which is a consequence of both population increase and urban activities. Furthermore, the area has hot and dry summers, mild to cold winters, and occasional rainfall, defining a semi-arid climate. This region's varied topography, which includes both agriculturally productive flat terrain and more hilly regions close to rivers, contributes to climatic changes, such as the impacts of increasing surface temperatures. It is located between the longitudes of 44°16'39" East and 44°23'10" East, as well as the latitudes of 33°23'00" North and 33°29'00" North. A part of the Tigris River passes through the study area. The study area also contains diverse plant cover distributed irregularly around the river and a different land cover, as in Fig. 1a and b.

### 2.2. Database

For this investigation, satellite data was used. Landsat-5 TM images for the years 2000 and Landsat-8 OLI/TIRS images for the year 2024 were collected from the USGS (<https://earthexplorer.usgs.gov/>), details of which can be found in Table 1. These images and data were then used for the necessary geostatistical and geospatial analysis. These images were collected over twenty-four years to comprehend the Baghdad province's chronological changes better. Before conducting the geo-special analysis, the images were adjusted using radiometric calibration and atmospheric correction.

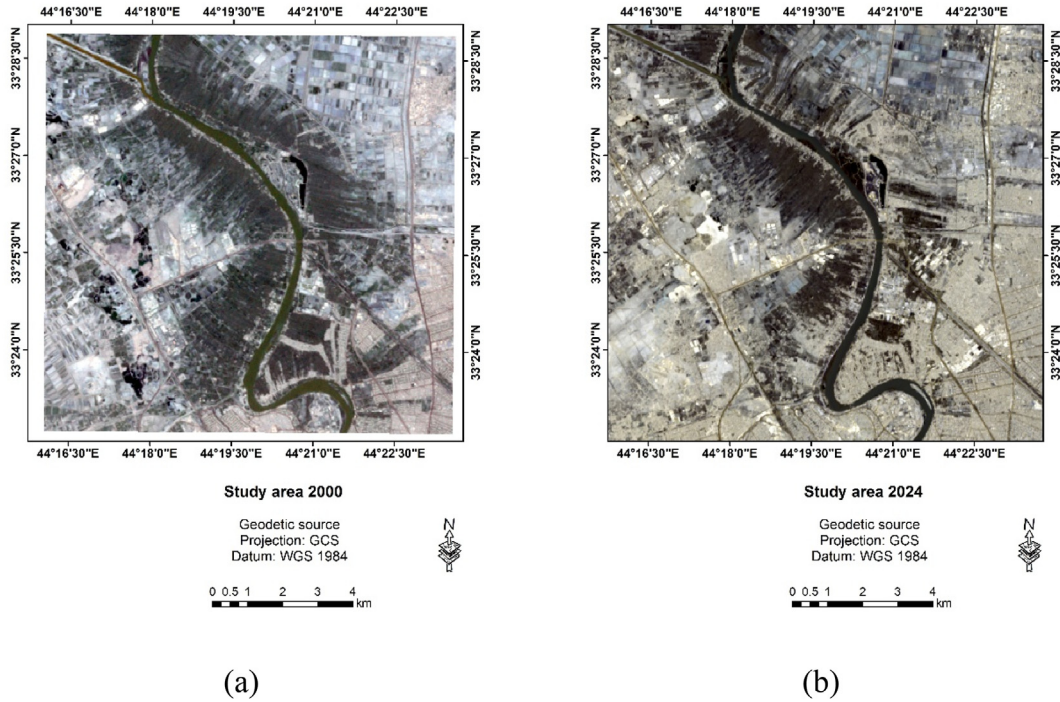


Fig. 1. Study area for the years (a) 2000 and (b) 2024.

Table 1. The study used satellite data.

No.	Satellite	Sensor	Path/Row	Date of acquisition	Resolution
1	Landsat 5	TM	168/38	19/09/2000	30 m
2	Landsat 8	OLI/TIRS	168/37	27/09/2024	30 m

There are no clouds in the study area, and the images have a resolution of 30 m.

### 2.3. Methods

Temperature data is collected by satellite sensors like Landsat and recorded as a DN between 0 and 255. Use the four-stage procedure below to transform these DNs into LST:

Computation of Brightness Temperature:

Digital numbers (DN) from Landsat thermal bands are converted to spectral radiance using the image information and the following method to calculate brightness temperature:

(A) Landsat TM and ETM + [15].

$$R\lambda = \left[ \frac{L_{max.\lambda} - L_{min.\lambda}}{Q_{calmax.} - Q_{calmin.}} \right] * [Q_{cal} - Q_{calmin.}] + L_{min.\lambda} \quad (1)$$

Where:

$R\lambda$  is the range of light that  $[W/(m^2 \times sr. \times \mu m)]$ .

$Q_{cal}$  is the numerical value assigned to a single pixel.

$L_{max}$  does the spectrum of light.

$L_{min}$  does the spectrum of light.

$Q_{cal} \max$  is a pixel's highest calibrated value.

$Q_{cal} \min$  the pixel with the lowest calibrated value.

(B) Landsat OLI [16].

$$R\lambda = [ML * Q_{cal}] + AL \quad (2)$$

Where:

$ML$  is a multi-band radiance signal where  $n$  is the number of bands.

$AL$  is the brightness; multiply by band  $n$ , where  $n$  is the number of bands.

Lastly, the formula calculates the brightness temperature [16].

$$Br.Temp. = \left[ \frac{k2}{\ln \left( \left( \frac{k1}{R\lambda} \right) + 1 \right)} \right] - 273 \quad (3)$$

Where:

$Br. Temp$  is the temperature in Celsius measured at the top of the atmosphere.

$K1$  and  $K2$  are the band conversion constants.

$K1$  value constant band 6 = 607.76.

$K2$  value constant band 6 = 1260.56.



(2) Landsat Normalized Difference Vegetation Index (NDVI) values may be calculated using the following formula [17–19]:

$$NDVI = \frac{(\rho.NIR - \rho.RED)}{(\rho.NIR + \rho.RED)} \quad (4)$$

Where:  $\rho.RED$  represents the red reflectance while  $\rho.NIR$  stands for the near-infrared reflectance.

(3) Computation of vegetation proportion ( $pr.$ ) by the following formula [18]:

$$pr. = \left[ \frac{NDVI - NDVI_{min.}}{NDVI_{max.} - NDVI_{min.}} \right]^2 \quad (5)$$

(4) Computation of Land Surface Emissivity ( $E$ ) as follows [20]:

$$E = (4 * 10^{-3}) * pr. + (986 * 10^{-1}) \quad (6)$$

(5) Finally, here is the formula to determine the LST value [18]:

$$LST = [Br.Temp. / (1 + (\lambda e. * Br.Temp. / p) * \ln(E))] \quad (7)$$

Where:

$$P = 14,380$$

$\lambda e$  is the length of the wavelength at which radiation is released (11.345  $\mu m$  for TM or ETM+ and 11.5  $\mu m$  for OLI) [20].

Based on Jenks' optimization approach, the natural breaks classification approach groups data into similar categories. Historically, when using the natural breaks method to define classes, the user (or cartographer) analyzed the attribute's distribution and determined where the necessary class breaks should occur [21]. Grouping data shows the greatest variation out groups and the least variation within each class utilizing natural breaks. ArcGIS software uses Jenks optimization, a statistical technique for grouping data values into sets, to take advantage of the logical breaks that occur in the data [22].

ArcGIS software uses this system as its standard approach to classification. This technique classifies data into comparable groups using an algorithm to find the data's discrete points in a histogram [23]. The values of the natural breaks are rounded to a number that is simpler to read and understand while still preserving the general pattern of the natural breaks that were originally there. These values are determined by the equation that is shown below [22]:

$$GVF = 1 - \frac{\sum_{j=1}^k \sum_{i=1}^{N_j} (z_{ij} - \bar{z}_j)^2}{\sum_{i=1}^{N_j} (z_{ij} - \bar{z}_j)^2} \quad (8)$$

Where:

GVF (Generalized Variance Function) = satisfactory fit for variance.

$z_{ij}$  = squared discrepancies from the average of the array.

$z_j$  = value of the squared difference between classes.

Creating an LST map is a multi-step process that requires merging and analyzing data from different spectral sources, as shown in the table. Each step contributes to improving the accuracy of the final information about LST. Fig. 2a and b shows the stages of preparing the LST map for 2000 and 2024 and includes many different analytical processes and spectral data, respectively.

### 3. Results and discussion

The study is helpful due to the details of changes in land cover through the years 2000 and 2024. It also illustrates the benefits of combining efficient GIS methods with readily available remotely sensed data for information extraction. Creating Land Surface Temperature (LST) maps relies on using satellite data and digital image processing to analyze and interpret thermal changes on the Earth's surface.

#### 3.1. Land surface temperature map 2000

The band 6 map is the first step in creating a map of the LST. At this stage, spectral data captured by satellites in the sixth band are used, as this band usually represents the wavelengths that respond to thermal changes, as in Fig. 3a. After obtaining the sixth band data, this data is converted into a radiation map. A radiation map shows the spatial distribution of radiant energy emitted from the Earth's surface. This map is crucial because it converts digital values recorded by satellites into physical units that can be used to calculate temperature, as in Fig. 3b.

The Kelvin temperature map represents the next stage of the processing process, where radiation values are converted into temperature values using appropriate physical equations. Kelvin temperature expresses the absolute temperature and is an important step in accurately understanding the temperature distribution on the Earth's surface, as in Fig. 3c. The final map is the LST map, which shows the spatial distribution of temperatures on the Earth's surface for the given year, in this case,

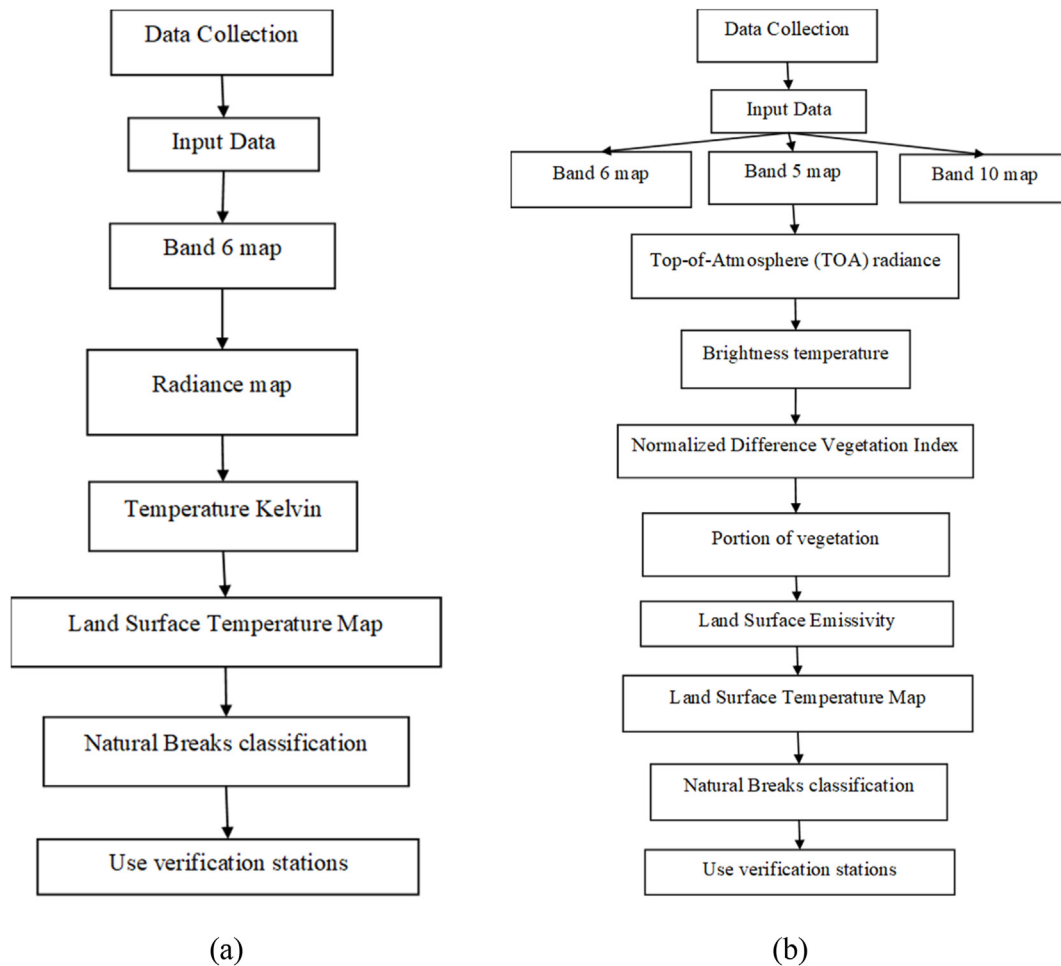


Fig. 2. General workflow diagram: (a) LST map 2000, (b) LST map 2024.

2000. This map is the ultimate tool for environmental, climate, and agricultural studies, providing valuable information about Thermal changes and their effects on different ecosystems, as in Fig. 3d.

### 3.2. Land surface temperature map 2024

**Band 4 map:** This band is used to determine the characteristics of plants and water, contributing to the analysis of environmental impacts on surface temperature, as in Fig. 4a.

**Band 5 map:** This band provides additional information on vegetation, rocks, and soil, which helps improve the accuracy of temperature calculations, as in Fig. 4b.

**Band 10 map:** This band is considered essential in measuring the thermal radiation emanating from the Earth's surface, and it is the key to calculating the LST, as in Fig. 4c.

**Top-of-Atmosphere (TOA) radiance:** This radiation calculates temperature changes due to

atmospheric effects, allowing raw data to be corrected and converted into accurate information about LST, as in Fig. 4d.

**Brightness temperature:** This step is vital because it represents the conversion of radiation data into actual temperature, which is the basis for determining the LST map, as in Fig. 4e.

**Normalized Difference Vegetation Index (NDVI):** Vegetation cover greatly affects LST. NDVI helps identify areas densely covered by vegetation, which helps adjust temperature data based on the effects of vegetation, as in Fig. 4f.

**Portion of vegetation:** This data helped improve the accuracy of the LST map by adjusting thermal radiation based on the percentage of vegetation cover, as in Fig. 4g.

**Land Surface Emissivity (LSE):** Surface emissivity is an important factor in calculating temperature, as it varies depending on the surface type (water, soil, plants) and directly affects the accuracy of the LST map, as in Fig. 4h.

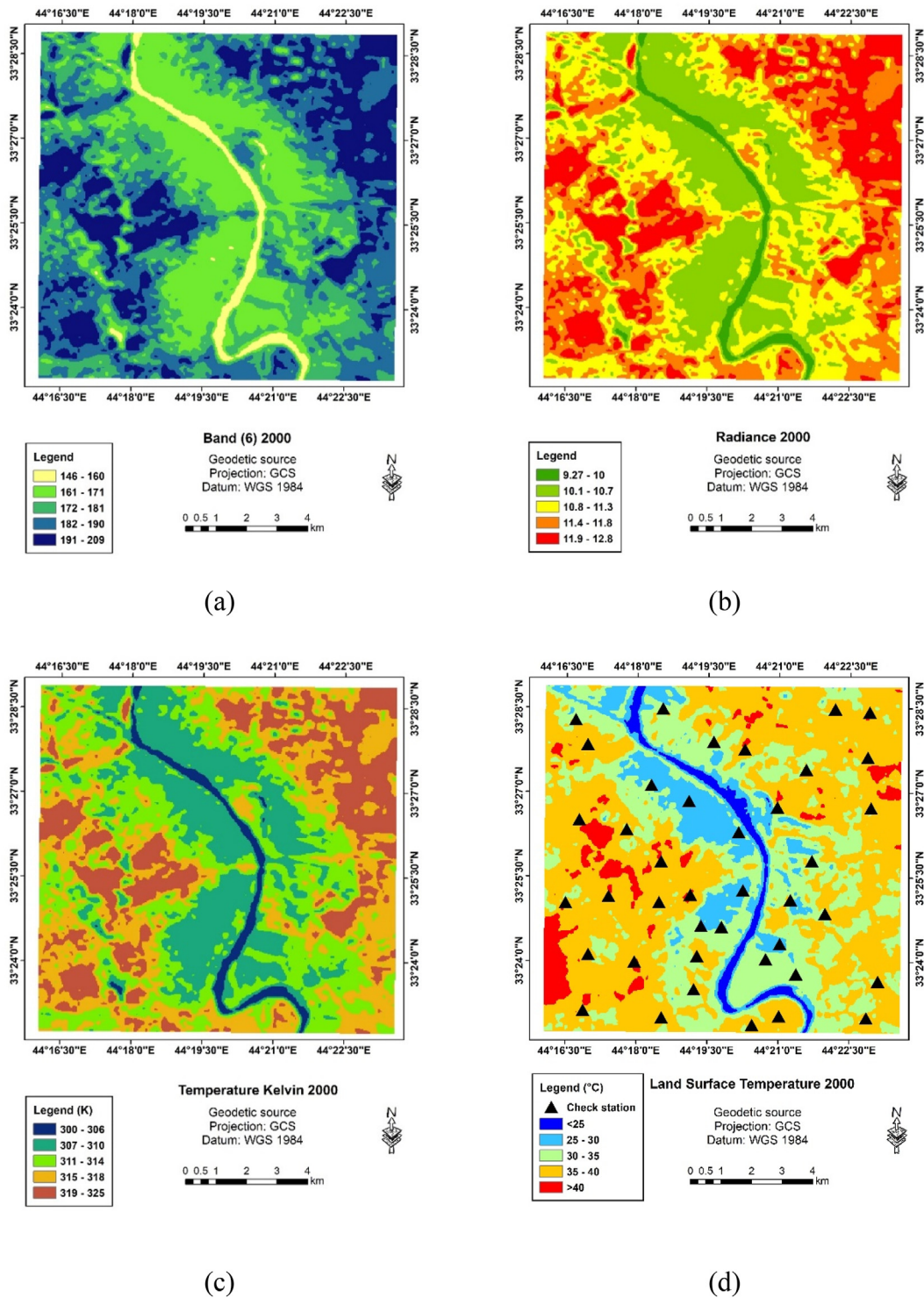
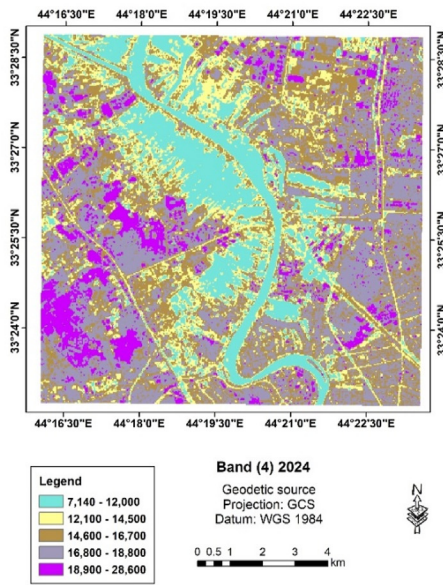


Fig. 3. Stages of creating a map of the Land Surface Temperature (LST) for the year 2000, (a) Band 6 map, (b) Radiance map, (c) Temperature kelvin map, (d) Land Surface Temperature map 2000.

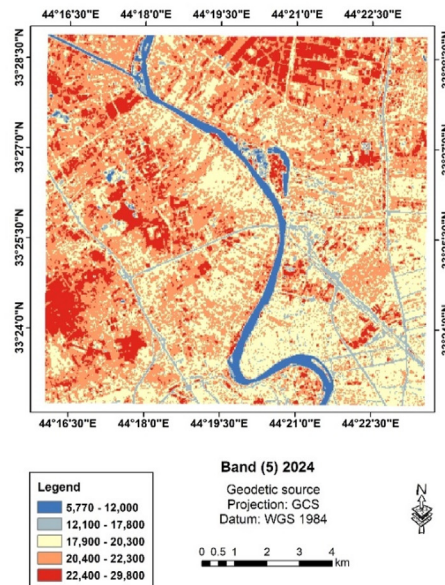
**LST map 2024:** This map provides a comprehensive and accurate view of temperatures on the Earth's surface for 2024, enabling scientists and

researchers to study climate and environmental changes and make decisions based on reliable information, as in Fig. 4i.

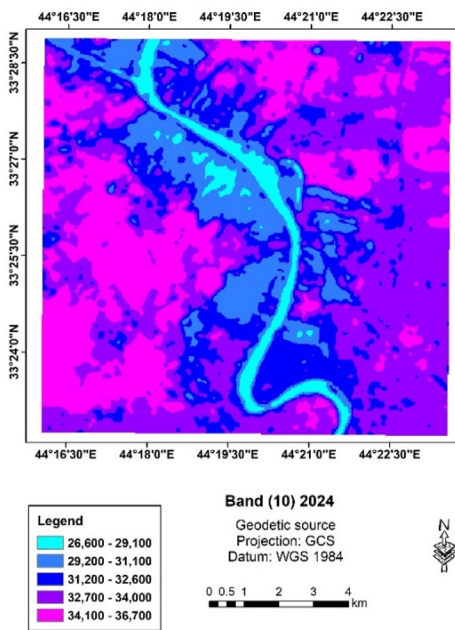




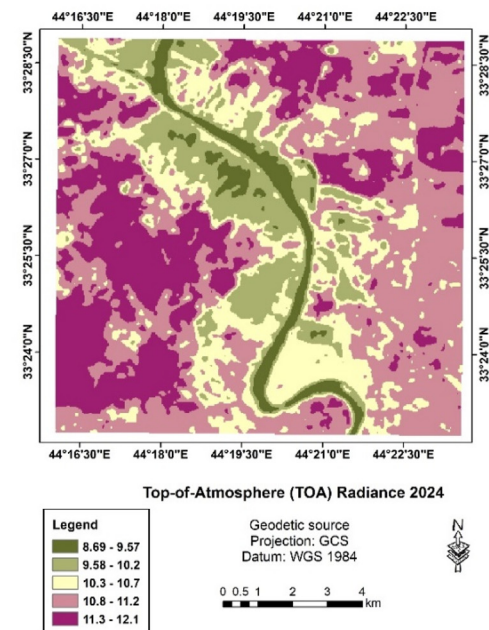
(a)



(b)



(c)



(d)

Fig. 4. Stages of creating a map of the Land Surface Temperature (LST) for the year 2024, (a) Band 4 map, (b) Band 5 map, (c) Band 10 map, (d) Top-of-Atmosphere (TOA) radiance, (e) Brightness temperature, (f) Normalized Difference Vegetation Index (NDVI), (g) Portion of vegetation, (h) Land Surface Emissivity (LSE), (i) Land Surface Temperature map 2024.

### 3.3. Comparison of results between LST map 2000 and LST map 2024

Table 2 provides data on land surface temperatures for 2000 and 2024 across 40 stations, with their geographic coordinates (Easting and Northing). The

stations cover various coordinates from north to south and east to west, indicating comprehensive coverage of the studied site. These coordinates help in analyzing climate changes at a precise local level. Almost all stations show a significant increase in LST from 2000 to 2024. Some stations show

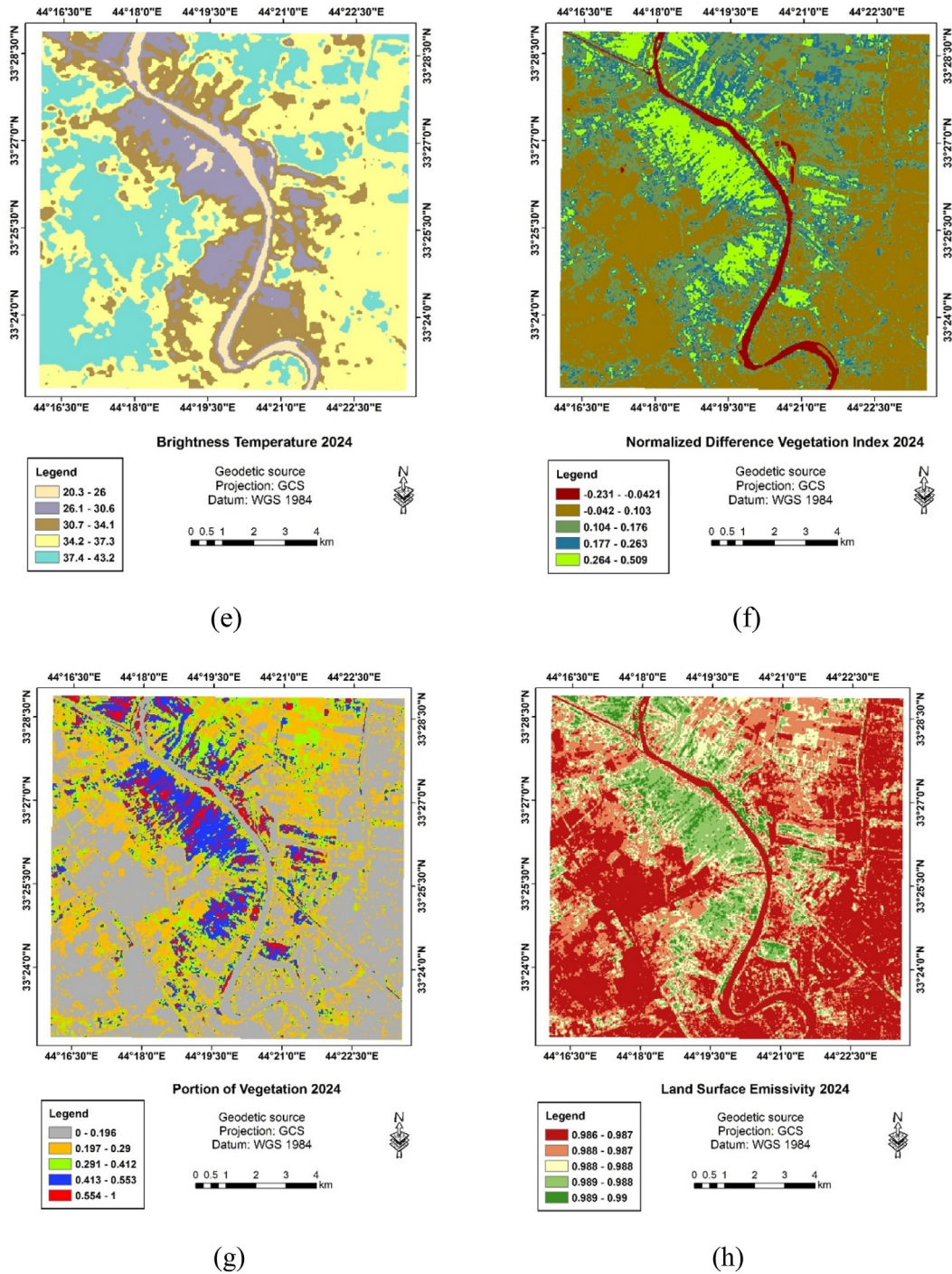
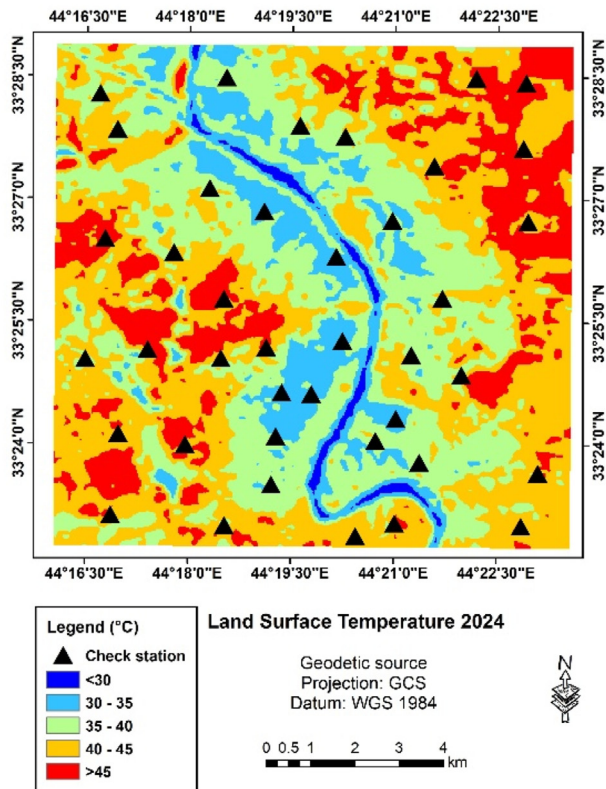


Fig. 4. (Continued)

significant increases of more than 10 °C, such as station 12, which rose from 35.69 °C in 2000 to 48.13 °C in 2024. Southern and eastern locations tend to have higher temperatures than other stations. Station 9, for example, rose from 41.14 °C to just 43.34 °C, compared to other stations that saw larger increases. Stations 12, 17, and 34 experienced

sharp increases, indicating intense local environmental changes that may warrant in-depth study to understand possible causes. The expected relationship between vegetation cover and LST was larger than between total vegetation cover. This could be because trees are more resistant to dry conditions that come with heatwaves, and the city's





(i)

Fig. 4. (Continued)

urbanization and industrialization have caused a rise in LST.

Table 3 presents the land surface temperature (LST) statistics for the studied area. RMSE is a measure of accuracy, and it represents the square root of the mean of the squares of the differences between the predicted values and the actual values. The lower the RMSE, the more accurate the forecasts. We find that the RMSE has increased slightly from 1.89 in 2000 to 1.98 in 2024, indicating a slight increase in the inaccuracy of the forecast data for 2024 compared to 2000. It can be noted that there is a significant increase in the average temperature from 34.76 °C in 2000 to 40.25 °C in 2024. This increase indicates a clear rise in temperatures over the past 24 years, which may indicate climate changes in the region.

We find that the maximum temperature increased from 41.14 °C in 2000 to 48.13 °C in 2024, which reinforces the idea that there is a significant increase in maximum temperatures in the studied region. We note that the minimum temperature increased from 26.29 °C in 2000 to 33.66 °C in 2024.

Table 2. Stations were observed on the final map data to calculate the land surface temperature.

Station	Easting (m)	Northing (m)	LST year 2000 (°C)	LST year 2024 (°C)
1	436,639	3,701,100	26.32	34.06
2	435,792	3,704,130	32.34	36.83
3	439,531	3,700,890	37.55	36.83
4	441,083	3,697,400	35.19	39.55
5	442,811	3,695,180	35.55	42.59
6	442,423	3,693,980	35.46	42.21
7	438,684	3,693,760	36.78	43.34
8	436,780	3,694,930	35.24	37.61
9	434,840	3,695,850	41.14	43.34
10	433,324	3,696,090	38.27	42.21
11	432,583	3,697,790	37.72	39.16
12	433,041	3,700,500	35.69	48.13
13	433,324	3,702,970	37.26	39.55
14	437,450	3,703,040	34.26	41.07
15	440,483	3,702,120	33.42	42.21
16	442,493	3,702,510	36.27	43.71
17	442,564	3,703,990	37.08	45.20
18	438,261	3,700,080	28.05	34.06
19	437,697	3,696,970	28.00	34.06
20	436,886	3,696,020	35.69	35.26
21	438,402	3,698,170	28.83	34.06
22	437,027	3,697,010	30.16	34.06
23	439,143	3,695,920	33.96	39.55
24	440,130	3,695,420	33.00	38.00
25	439,601	3,696,410	26.29	33.66
26	439,954	3,697,860	34.73	36.83
27	440,659	3,699,130	33.02	39.16
28	434,593	3,700,180	32.68	41.07
29	435,722	3,699,130	38.40	45.20
30	435,651	3,697,790	36.83	41.07
31	433,994	3,698,000	38.42	45.57
32	438,473	3,702,790	37.79	38.78
33	435,404	3,701,630	30.62	39.55
34	436,674	3,698,030	40.09	45.93
35	439,566	3,694,050	37.52	44.46
36	435,722	3,694,010	35.44	39.93
37	433,147	3,694,260	37.92	44.46
38	432,936	3,703,780	34.59	38.39
39	441,435	3,704,100	37.35	45.20
40	442,599	3,700,850	35.37	44.08

Table 3. Summary statistics of LST for the study area.

LST	RMSE	Mean	Max	Min	STD
LST year 2000 (°C)	1.89	34.76	41.14	26.29	3.57
LST year 2024 (°C)	1.98	40.25	48.13	33.66	3.92

This increase in minimum values reflects that temperatures did not decrease much during cold periods, reinforcing the global warming hypothesis. The standard deviation measures the dispersion around the mean. We note a slight increase in the standard deviation from 3.57 in 2000 to 3.92 in 2024, which indicates an increase in the variability of temperatures around the mean, which may reflect greater fluctuations in temperatures in the region. This analysis clearly shows an increase in surface

temperatures in the studied region between 2000 and 2024, with an increase in the mean, maximum, and minimum, as well as a slight increase in dispersion and imprecision. These results support hypotheses related to climate change and its effects on surface temperatures.

The maps are shown in Fig. 5 show the distribution of land surface temperatures (LST) in the northeastern region of Baghdad province in 2000 and 2024. By comparing the two maps, it can be noted that there are significant changes in the distribution of surface temperatures between 2000 and 2024:

1. Spatial changes: Some places had unusually high temperatures in 2000, suggesting either a lack of urbanization or a change in land use. The geographical extent of high-temperature zones clearly increases in 2024, suggesting either a shift in land cover or the growth of cities.
2. Temporal changes: Variations in the two maps show how different geographical and meteorological variables affected land surface temperatures during the research period. Alterations in land use or the loss of plant cover as a result of urbanization are indicated by changes in surface temperature.
3. Environmental impact: Surface temperature increases seen on the 2024 map indicate further population at the cost of natural vegetation,

which can have detrimental effects on the environment, such as a worsening of the urban heat island effect.

Fig. 6 Compares LST for the years 2000 and 2024. Comparing LST between two periods is essential to climate and environmental change research, helping to understand climate changes over time. The increase in temperature in most regions can be seen by the different colors representing different LST values. There is a general increase in LST between the years 2000 and 2024. This pattern is consistent with tabular data indicating significant increases in LST across almost all stations.

Rapid change and new possibilities are on the horizon for the area, resulting in the need for innovative strategies. In addition, An effective agricultural strategy may be developed using the approach and conclusions of this study to mitigate the harm to agricultural fields during a certain period. Natural and human-caused variables, such as climate, elevation, population growth, and pressure on natural resources, all resulted in severe changes in the land cover of the studied region. Future events and land cover changes may be monitored and predicted with the assistance of this study. Policymakers and decision-makers might use the results of this study to reduce excessive usage of natural resources. This work provided evidence that LST may be derived using

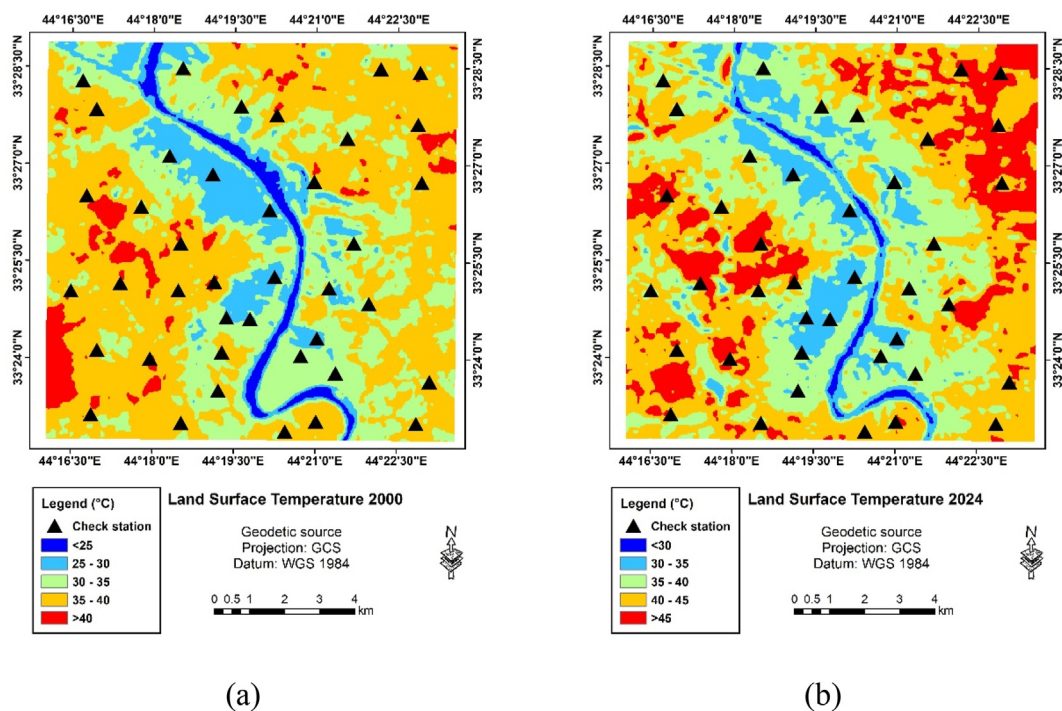


Fig. 5. Results of final maps: (a) LST 2000 and (b) LST 2024.

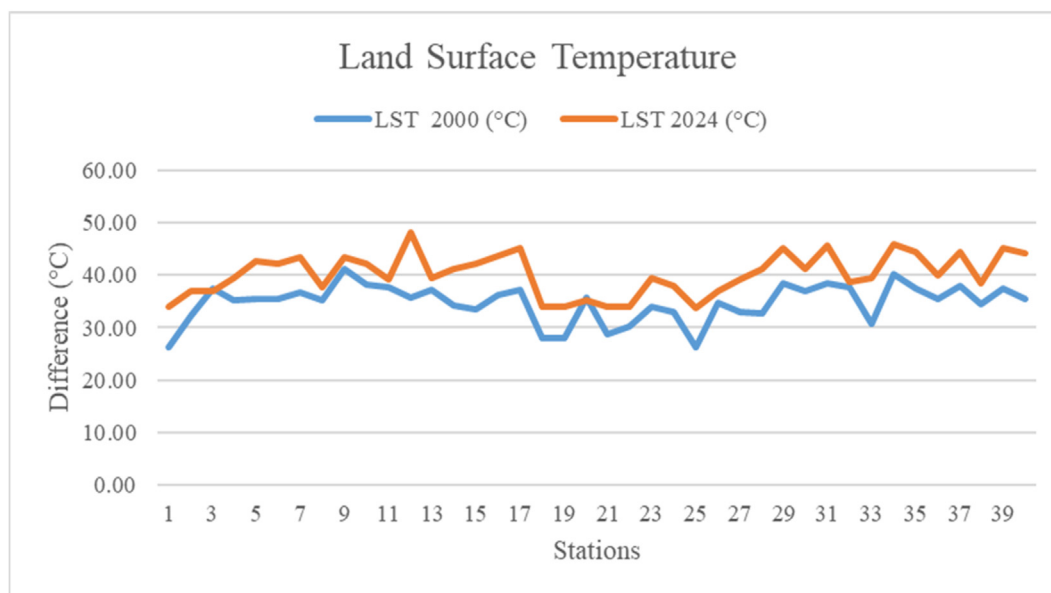


Fig. 6. Comparing LST for the year 2000 and 2024.

remote sensing and GIS, which opens up new possibilities for environmental research and studies. Additional research should include estimating LST in each city and validating these estimates with observations made in the actual environment.

#### 4. Conclusions

This particular type of study could assist in creating sustainable social, ecological, and environmental policies and practices. This study helps stakeholders and decision-makers focus on future change by detecting areas of quick land use change. In this research for the study area between 2000 and 2024, the following can be concluded:

1. Significant increase in surface temperatures: From 2000 to 2024, the statistics showed that the northeastern portion of Baghdad province had significantly higher average surface temperatures. With an increase of around 5.49 °C, the average temperature rose from 34.76 °C in 2000 to 40.25 °C in 2024.
2. Spatio-temporal variation: Variation in the rise among stations is clearly seen in the data from the tables. Geographical distribution 12 is one such location that saw temperatures surge dramatically, from 35.69 °C in 2000 to 48.13 °C in 2024. Meanwhile, in other stations, such as Station 25, the increase was less severe, from 26.29 °C to 33.66 °C.
3. Variation in maximum and minimum values: In contrast to 2000, when maximum temperatures

ranged from 26.29 °C to 41.14 °C, the minimum temperature in 2024 is 33.66 °C and the maximum temperature is 48.13 °C. This reflects substantial changes in the local climate and possible effects on the environment and human activities.

4. Root Mean Square Error (RMSE): The root-mean-squared error (RMSE) rose from 1.89 in 2000 to 1.98 in 2024, suggesting a small but noticeable rise in the data's variability throughout the years.
5. Potential Environmental Impact: The region's negative environmental impacts, like the urban heat island effect and vegetation cover degradation, could worsen as a result of these increasing temperatures; therefore, steps should be taken to reduce these impacts, and suitable environmental sustainability policies should be developed.

#### Ethics information

This research complies with the ethical information for conducting scientific studies.

#### Data availability statement

Publicly available data.

#### Author contribution

The author declares sole responsibility for all aspects of this research. This includes data collection, analysis, and interpretation, as well as the drafting and revision of the manuscript.



## Funding

No Funding.

## Conflict of interest

No conflicts of interest related to this work.

## Acknowledgment

This research was conducted independently by the author without any external funding or financial support. No grant IDs or funding sources are applicable for this study.

## References

- [1] Al-Saedi ASJ, Kadhum ZM, Jasim BS. Land use and land cover analysis using geomatics techniques in amara city. *Ecol Eng* 2023;9:161–9. <https://doi.org/10.12912/27197050/173211>.
- [2] Jasim BS, Jasim OZ, AL-Hameedawi AN. A review for vegetation vulnerability using artificial intelligent (AI) techniques. *AIP Conf Proc* 2024;3092(1). <https://doi.org/10.1063/5.0199653>.
- [3] Nations U. World population prospects: the 2017 revision, key findings and advance tables. *Dep Econ Soc Aff PD* 2017; 46(1). New York United Nations.
- [4] Svirejeva-Hopkins A, Schellnhuber HJ, Pomaz VL. Urbanised territories as a specific component of the global carbon cycle. *Ecol Model* 2004;173(2–3):295–312. <https://doi.org/10.1016/j.ecolmodel.2003.09.022>.
- [5] Alexander C. Normalised difference spectral indices and urban land cover as indicators of land surface temperature (LST). *Int J Appl Earth Obs Geoinf* 2020;86(July 2019):102013. <https://doi.org/10.1016/j.jag.2019.102013>.
- [6] U RJ, Abah IA. Derivation of land surface temperature (Lst) from Landsat 7 & 8 imageries and its relationship with two vegetation indices (Ndvi and Gndvi). *Int J Res Granthaalayah* 2019;7(2):108–20. <https://doi.org/10.29121/granthaalayah.v7.i2.2019.1013>.
- [7] Dodge R, Congalton RG. Meeting environmental challenges with remote sensing imagery. 2013.
- [8] Bhatta B. Research methods in remote sensing. Springer; 2013.
- [9] Verbesselt J, Hyndman R, Newnham G, Culvenor D. Detecting trend and seasonal changes in satellite image time series. *Remote Sens Environ* 2010;114(1):106–15. <https://doi.org/10.1016/j.rse.2009.08.014>.
- [10] Ochola EM, Fakharizadehshirazi E, Adimo AO, Mukundi JB, Wesonga JM, Sodoudi S. Inter-local climate zone differentiation of land surface temperatures for Management of Urban Heat in Nairobi City, Kenya. *Urban Clim* 2020;31:100540. <https://doi.org/10.1016/j.uclim.2019.100540>.
- [11] Kadhum ZM, Jasim BS, Obaid MK. Change detection in city of hilla during period of 2007-2015 using remote sensing techniques. *IOP Conf Ser Mater Sci Eng* 2020;737(1):12228. <https://doi.org/10.1088/1757-899X/737/1/012228>.
- [12] Kadhum ZM, Jasim BS, Al-saedi ASJ. Improving the spectral and spatial resolution of satellite image using geomatics techniques improving the spectral and spatial resolution of satellite image using geomatics techniques, 40011; April, 2023. <https://doi.org/10.1063/5.0138463>.
- [13] Jasim BS, Al-Bayati ZMK, Obaid MK. Accuracy of horizontal coordinates of cadastral maps after geographic regression and their modernization using gis techniques. *Int J Civ Eng Technol* 2018;9(11):1395–403.
- [14] Jasim BS, Al-Saedi ASJ, Kadhum ZM. Using remote sensing application for verification of thematic maps produced based on high-resolution satellite images. *AIP Conf Proc* 2024; 3092(1). <https://doi.org/10.1063/5.0199654>.
- [15] Zaharaddeen I, Baba II, Zachariah A. Estimation of land surface temperature of Kaduna metropolis, Nigeria using Landsat images. *Sci World J* 2016;11(3):36–42.
- [16] Landsat U. Product guide-using the USGS Landsat 8 product; Resource document USGS. 82014; 2016.
- [17] Jasim B, Jasim OZ, AL-Hameedawi AN. Monitoring change detection of vegetation vulnerability using hotspots analysis. *IJUM Eng J* 2024;25(2):116–29. <https://doi.org/10.31436/iiumej.v25i2.3030>.
- [18] Suresh S, Mani K. Application of remote sensing in understanding the relationship between NDVI and LST. *Int J Res Eng Technol* 2017;6(2).
- [19] Krieglner FJ. Preprocessing transformations and their effects on multispectral recognition. In: Proceedings of the sixth international symposium on remote sensing of environment; 1969. p. 97–131.
- [20] Agbor CF, Makinde EO. Land surface temperature mapping using geoinformation techniques. *Geoinformatics FCE CTU* 2018;17(1):17–32. <https://doi.org/10.14311/gi.17.1.2>.
- [21] Slocum TA, McMaster RM, Kessler FC, Howard HH, McMaster RB. Thematic cartography and geographic visualization. 2008.
- [22] Baz I, Geymen A, Er SN. Development and application of GIS-based analysis/synthesis modeling techniques for urban planning of Istanbul Metropolitan Area. *Adv Eng Software* 2009;40(2):128–40. <https://doi.org/10.1016/j.advengsoft.2008.03.016>.
- [23] Jenks GF, Caspall FC. Error on choroplethic maps: definition, measurement, reduction. *Ann Assoc Am Geogr* 1971;61(2): 217–44. <https://doi.org/10.1111/j.1467-8306.1971.tb00779.x>.